RESEARCH PAPER

Cell Adhesion & Migration 9:6, 502–512; November/December 2015; © 2015 Taylor & Francis Group, LLC

Inhibition of cell adhesion by phosphorylated Ezrin/Radixin/Moesin

Kouichi Tachibana[1,*], Seyed Mohammad Ali Haghparast[2], and Jun Miyake[2]

[1]Biomedical Research Institute; National Institute of Advanced Industrial Science and Technology (AIST); Tsukuba, Ibaraki, Japan; [2]Department of Mechanical Science and Bioengineering; Graduate School of Engineering Science; Osaka University; Toyonaka, Osaka, Japan

Keywords: cell adhesion, cell rounding, dephosphorylation, ERM, phosphorylation, rigidity, spherical cell shape

Abbreviations: Ab, antibody; AF, Alexa fluor; AFM, atomic force microscopy; Blebbi, Blebbistatin; Cal-A, Calyculin A; ERM, Ezrin/Radixin/Moesin; FAK, foal adhesion kinase; FERM, four point one ERM; Moesin-TD, Moesin Thr558 to Asp mutant; Moesin-wt, wild type Moesin; phospho-ERM, C-terminal Thr phosphorylated ERM proteins; PLL, poly-L-lysine; SDF-1, Stromal Cell-derived Factor 1; Sta, Staurosporine.

Altered phosphorylation status of the C-terminal Thr residues of Ezrin/Radixin/Moesin (ERM) is often linked to cell shape change. To determine the role of phophorylated ERM, we modified phosphorylation status of ERM and investigated changes in cell adhesion and morphology. Treatment with Calyculin-A (Cal-A), a protein phosphatase inhibitor, dramatically augmented phosphorylated ERM (phospho-ERM). Cal-A-treatment or expression of phospho-mimetic Moesin mutant (Moesin-TD) induced cell rounding in adherent cells. Moreover, reattachment of detached cells to substrate was inhibited by either treatment. Phospho-ERM, Moesin-TD and actin cytoskeleton were observed at the plasma membrane of such round cells. Augmented cell surface rigidity was also observed in both cases.

Meanwhile, non-adherent KG-1 cells were rather rich in phospho-ERM. Treatment with Staurosporine, a protein kinase inhibitor that dephosphorylates phospho-ERM, up-regulated the integrin-dependent adhesion of KG-1 cells to substrate.

These findings strongly suggest the followings: (1) Phospho-ERM inhibit cell adhesion, and therefore, dephosphorylation of ERM proteins is essential for cell adhesion. (2) Phospho-ERM induce formation and/or maintenance of spherical cell shape. (3) ERM are constitutively both phosphorylated and dephosphorylated in cultured adherent and non-adherent cells.

Introduction

Most metazoan cells are adhered to adjacent cells and/or connective tissues such as basal membrane. These adhered cells show various morphologies, but have flat surface areas at the attachment sites to substrate and/or to the other cells. Meanwhile, non-adherent cells such as leukocytes and oocytes are spherical and maintain such round shape unless attached to other cells. Adherent cells also become spherical during mitosis and when detached from substrate by trypsinization. Thus, most metazoan cells adopt spherical shape and maintain this morphology when not attached to substrate or to other cells. At the same time, they should have machineries to cancel such spherical shape when attached to substrate or other cells.

Although the mechanisms to generate and/or maintain spherical cell shape have not been fully revealed, ERM proteins seem to be the key players. Non-adherent cells such as T lymphocytes are spherical and have microvilli on their surface. Previous studies showed that dephosphorylation of ERM proteins and shift of their subcellular localization were accompanied by cell shape changes. Chemokines induced morphological changes including polarization, membrane ruffling, loss of spherical shape and microvilli in T lymphocytes.[1,2] ERM proteins were localized to uropods induced by chemokine treatment in T lymphoblasts.[1] Treatment with Stromal Cell-derived Factor 1 (SDF-1) caused rapid dephosphorylation of ERM proteins in peripheral T lymphocytes, while expression of phospho-mimetic Moesin mutant delayed SDF-1-induced microvilli collapse.[2] Meanwhile, T cell receptor signaling induced cell shape change and binding to antigen presenting cells. ERM proteins were dephosphorylated and excluded from immunological synapse by T cell receptor signaling.[3,4] These reports strongly suggested the involvement of phosphorylated ERM proteins in maintaining spherical cell shape and microvilli in T lymphocytes.

ERM are highly conserved cytoplasmic proteins. At least one family protein is found in all sequenced metazoans.[5,6] Each ERM protein contains a conserved FERM (four point one, ERM) domain in its N-terminal and an actin-binding domain in its C-terminal.[5,7] FERM domain is considered as the binding site for membrane components, phosphatidyl-inositide

*Correspondence to: Kouichi Tachibana; Email: kouichi-tachibana@aist.go.jp
Submitted: 07/07/2015; Revised: 09/11/2015; Accepted: 10/22/2015
http://dx.doi.org/10.1080/19336918.2015.1113366

4,5-bisphosphate and cytoplasmic domain of certain transmembrane proteins such as CD43, CD44 and ICAMs.[1,8-10] In closed and inactive conformation, FERM and C-terminal domains intramolecularly interact and mask each other's binding sites to other molecules.[6,11-13] When this conformation is opened up, ERM proteins can bind to membrane components and actin cytoskeleton via their FERM domain and C-terminal, respectively.[7,14,15] The mechanisms underlying these alternative conformational changes have not been fully revealed yet. However, phosphorylated Thr residue close to the C-terminal actin-binding site is a potent marker for the opened structure.[11,13,16,17] This Thr residue such as human Moesin T558 is surrounded by a sequence conserved among ERM proteins. Development of phospho-specific antibodies against this sequence containing phosphorylated Thr residue enabled identification of ERM proteins with phosphorylated Thr residue at this site (phospho-ERM).[18] Studies using such antibodies showed membarne localization of phospho-ERM and co-localization with actin cytoskeleton.[2,5,19,20] Thus, phospho-ERM represent active form of ERM proteins and function as cross-linkers between the plasma membrane and actin cytoskeleton.

Unlike non-adherent cells, adherent cells are flat and spread when attached to substrate during cell culture. However, adherent cells become temporarily round during mitosis and when detached from substrate. Among these cell shape changes in adherent cells, ERM proteins have been shown to play crucial roles in mitotic cell rounding. Moesin, which is the only ERM protein in Drosophila, is essential for cell rounding during mitosis. [21,22] Phosphorylated Moesin was observed at the plasma membrane of round mitotic cells and knocking down *Moesin* resulted in impaired cell body retraction during mitosis. Knocking down *Slik*, the gene encoding a protein kinase that phosphorylates Moesin, inhibited cell rounding as well. Thus, phosphorylated Moesin appear to be responsible for cell rounding of Drosophila adherent cells during mitosis. However, changes in phospho-ERM upon cell detachment and reattachment during tissue culture have not been studied yet.

We have reported that expression of cell surface mucin, CD43 or CD34, results in cell rounding, microvillous formation, and inhibition of cell adhesion to substrate in HEK293T cells.[23,24] Extracellular parts of mucins are highly *O*-glycosylated, and their cleavage augmented integrin-mediated reattachment of cells to substrate, indicating the inhibitory role of *O*-glycans in cell adhesion. These cell surface mucins are highly expressed in leukocytes, suggesting their roles in keeping leukocytes in suspended state by inhibiting cell adhesion. Meanwhile, expression of such mucin induced phosphorylation of ERM proteins in HEK293T cells.[23,24] ERM phosphorylation may be responsible for cell shape change and inhibition of cell adhesion in mucin-expressing HEK293T cells.

Besides mucin expression, we analyzed phosphorylation status of ERM proteins in HEK293T cells after detachment by trypsinization. We found that keeping cells unattached to substrate augmented phospho-ERM. Such augmented phospho-ERM decreased by the integrin-mediated cell adhesion.[23] These observations indicate: (i) phosphorylation of ERM upon cell detachment in adherent cells and (ii) dephosphorylation of ERM proteins upon cell adhesion to substrate. Phospho-ERM in detached cells is regarded to be involved in the formation and/or maintenance of spherical cell shape as well.

In this article, we modified phosphorylation status of ERM proteins and observed the subsequent alterations in cell shape, cell adhesion to substrate, and cell surface rigidity. These observations not only depicted the roles of phospho-ERM in cell shape formation and regulation of cell adhesion, but also suggested potential mechanisms for such events.

Results

Cell shape change, ERM phosphorylation, and inhibition of cell adhesion by Calyculin A treatment

We previously reported that inhibition of cell adhesion augmented phosphorylated ERM proteins (phospho-ERM), while cell adhesion to substrate decreased phospho-ERM.[23] To investigate cellular events caused by phospho-ERM, we treated adherent cells with protein phosphatase inhibitors and observed their effects on cell shape. Among tested inhibitors, Calyculin A (Cal-A) induced cell rounding in NIH3T3 and HEK293T cells when added to culture media at the concentration of 10 nM or more (**Fig. 1A** and Supple 1A). Within 30 min after Cal-A addition, more than half of NIH3T3 cells lost spread shape and became round. Not only cell bodies were retracted, bleb-like structures were observed on the surface of Cal-A-treated cells. To investigate ERM phosphorylation, cells were harvested at several time points after Cal-A addition and subjected to immunoblot analysis with anti-phospho-ERM antibody (Ab). As demonstrated in **Figure 1B** and Supple 1B, dramatic increase of phospho-ERM was observed over time after Cal-A addition.

To further study the relation between cell rounding and ERM phosphorylation, we modified Cal-A-induced ERM phosphorylation by Staurosporine, a powerful kinase inhibitor. NIH3T3 cells were incubated for 30 min with 50 nM Staurosporine, and then incubated with Cal-A. As a result, Staurosporine treatment partially inhibited Cal-A-induced cell shape change (**Fig. 1C** and Supple 2). Staurosporine treatment also decreased phospho-ERM in both Cal-A-treated and untreated cells (**Fig. 1D**). These findings indicate that: (i) phospho-ERM should be kept dephosphorylated by protein phosphatases that are inhibited by Cal-A in these adherent cells; (ii) ERM proteins are phosphorylated by protein kinases that are inhibited by Staurosporine in these cells; (iii) cell shape changes by Cal-A treatment, retraction of cell bodies and following cell rounding, correspond with the increase of phospho-ERM.

Since spread adherent cells became round by Cal-A treatment, we investigated the effect of Cal-A on the reattachment of trypsinized cells. Cal-A-preinucubated NIH3T3 cells were trypsinized and re-incubated for 1h with 10 nM Cal-A. After incubation, unattached cells were separated by flushing and counted, while reattached cells were imaged. As demonstrated in **Figure 1E and F**, Cal-A-treatment strongly inhibited reattachment of NIH3T3 cells to substrate. Similar inhibition of cell adhesion was observed

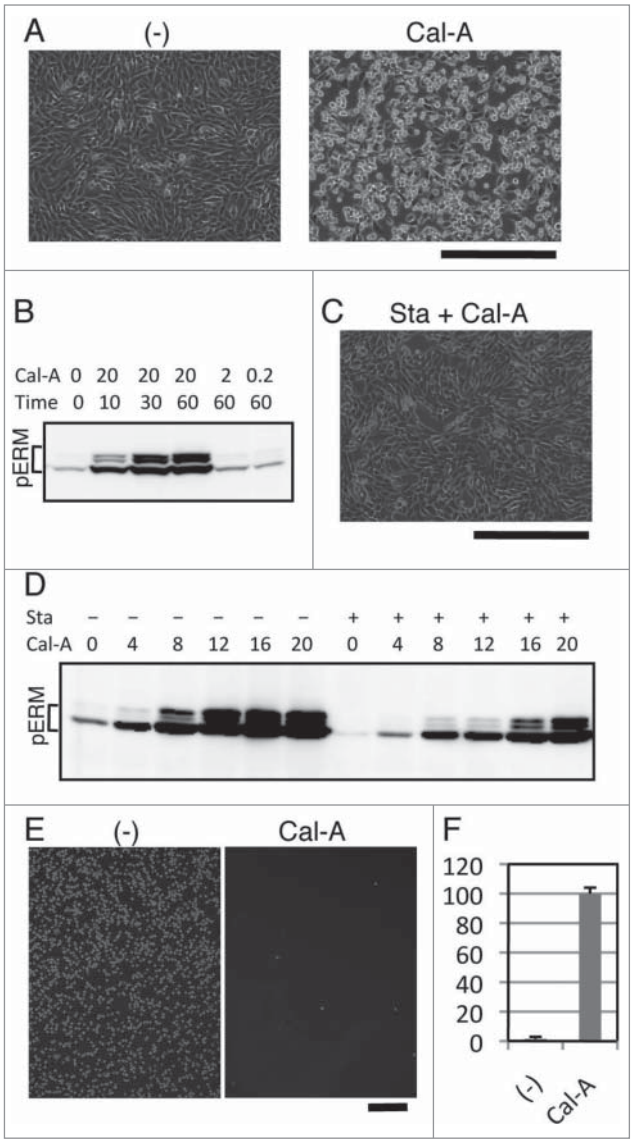

Figure 1. Effect of Calyculin A (Cal-A) on cell shape, ERM phosphorylation and inhibition of cell reattachment in NIH3T3 cells. (**A**) Cal-A treatment induced cell rounding in NIH3T3 cells. Cell bodies of flat cells were retracted within 30 min after incubation with 20 nM Cal-A. Magnification: x100. Scale bar: 400 μm. (**B**) Immunoblotting with anti-phospho-ERM Ab. Detection of phosphorylated ERM proteins (pERM) dramatically increased over time after the addition of Cal-A. Concentration of Cal-A: nM, time: min. (**C**) Suppression of Cal-A-induced NIH3T3 cell rounding by Staurosporine (Sta). Image of cells incubated for 30 min with 10 nM Cal-A after 50 nM Staurosporine pretreatment is shown. Staurosporine pretreatment delayed Cal-A-induced cell rounding. Magnification: x100. Scale bar: 400 μm. (**D**) Suppression of Cal-A-induced ERM phosphorylation by Staurosporine. Pretreatment with 50 nM Staurosporine was described by +, while concentrations of Cal-A (nM, 1h incubation) were also described. Staurosporine decreased phospho-ERM in Cal-A-treated and untreated cells. E: Inhibition of cell reattachment to substrate by Cal-A treatment. Detached NIH3T3 cells were re-incubated with or without 10 nM Cal-A then washed. Images of cells remained attached after wash are demonstrated. Magnification: x40. Scale bar: 400 μm. F: Ratios of unattached cells per total cells are demonstrated by percentage.

in HEK293T cells (Supple 1C). Moreover, unattached Cal-A-treated HEK293T cells eventually attached to substrate after removal of Cal-A (Supple 1C). Thus, Cal-A-treated cells with highly phosphorylated ERM proteins were not adhesive to substrate.

Influence of Moesin mutant on cell shape and adhesion

Although Cal-A treatment significantly affected cell shape, adhesion and ERM phosphorylation, many proteins other than ERM could be phosphorylated by Cal-A treatment.[25,26] To obtain more direct evidence for the role of phospho-ERM, we analyzed the effect of phospho-mimetic ERM mutant on cell shape and adhesion by developing an expression vector that coded a human Moesin Thr558 to Asp mutant (Moesin-TD). Human Moesin Thr558 is the conserved phosphorylation site among ERM family proteins, and Moesin-TD is considered as a mutant that mimics phospho-Thr558 Moesin. Wild-type Moesin (Moesin-wt) or Moesin-TD was expressed in HEK293T cells by vector transfection, and the effects of Moesin expression were investigated. Transfected cells were visualized by the expression of GFP whose gene was transcribed from the same vector. First, we investigated alterations of cell shape by Moesin expression. As demonstrated in **Figure 2A**, many round GFP+ cells were observed in pCGFP-Moesin-TD transfectants. A few round GFP+ cells were observed in pCGFP-Moesin-wt transfectants, while very few round GFP+ cells were observed in pCGFP transfectants. Ratio of round cells was much higher in Moesin-TD transfectants than in GFP-alone transfectants.

Next, to investigate the effect of expressed Moesin on cell adhesion, transfectants were trypsinized and allowed to reattach. As demonstrated in **Figure 2B**, less GFP+ cells attached to substrate in Moesin-TD transfectants than those in GFP-alone transfectants. To digitize the effect of Moesin-TD on cell reattachment, GFP+ cells per total cells in transfectants were determined in attached (**Fig. 2B**) and whole cells. As summarized in **Table 1**, less than half of GFP+ cells reattached to substrate in Moesin-TD transfectants, while most GFP+ cells reattached in GFP-alone transfectants. To further demonstrate the difference, both reattached and unattached cells were analyzed by flowcytometry. In Moesin-TD transfectants and Moesin-wt transfectants, high expression of GFP was observed in unattached cells, while lower or no expression of GFP was observed in attached cells (**Fig. 2C**). This result further suggested that higher expression of either Moesin-TD or Moesin-wt tended to inhibit reattachment of transfectants to substrate. Thus, expression of Moesin-TD inhibited reattachment of cells to substrate, while expression of Moesin-wt did it partially.

Expression of Moesin in these transfectants was investigated by immunoblot analysis with anti-ERM and anti-phospho-ERM Abs. Augmented expression of Moesin was identified as 75 kDa bands by anti-ERM Ab in Moesin-wt or Moesin-TD transfectants compared to non-transfectants (**Fig. 2D**). Meanwhile, no difference was observed in 80 kDa bands of Ezrin and Radixin in transfectants. Meanwhile, a dramatically augmented 75 kDa band was detected by anti-phospho-ERM Ab in Moesin-TD transfectants compared to non-transfectants, while the band in

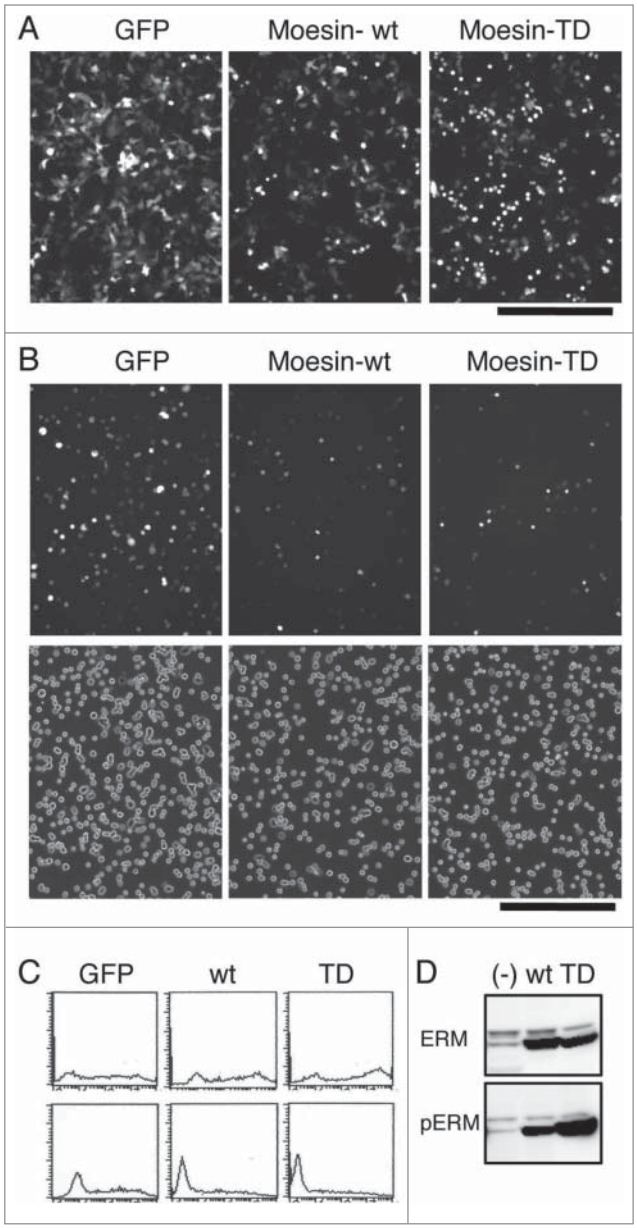

Figure 2. Cell rounding and inhibition of cell adhesion by the expression of Moesin-TD in HEK293T cells. (**A**) Rounding of HEK293T cells by Moesin-TD expression. Fluorescent images of transfectants 44h after transfection are demonstrated. GFP+ round cells/total GFP+ cells ratio for GFP-alone, Moesin-wt, Moesin-TD in these images was 4.3%, 9.2%, 35.4%, respectively. Magnification: x100. Scale bar: 200 μm. (**B**) Effect of expressed Moesin on HEK293T cell reattachment. Up: fluorescent images of reattached GFP+ cells after washing. Down: phase contrast images. Magnification: x100. Scale bar: 200 μm. (**C**) Flowcytometry of reattached and unattached Moesin transfectants. Expression of GFP in reattached cells (lower panel) and unattached cells (upper panel) was analyzed by flowcytometry after reattachment to substrate. High expression of GFP in unattached cells and low or no expression of GFP in attached cells were observed in Moesin-TD or wild-type Moesin transfectants. Horizontal axis: FL1. Vertical axis: cell count. (**D**) Immunoblot analysis of transfectants. Lysates of transfectants were analyzed by immunoblotting with anti-ERM and anti-phospho-ERM Abs.

Table 1. Effect of Moesin expression on the reattachment of HEK293T cells. GFP+ cells/total cells before wash represents the ratio of GFP+ transfectants. GFP+ cells/total cells after wash (**Fig. 2B**) represents the ratio of GFP+ transfectants attached to substrate per total attached cells. GFP+ after wash/GFP+ before wash reflects the effect of transfection on cell adhesion. Each number is shown by percentage.

	GFP	WT	TD
GFP+/total(Before)	38.8	29.2	36.1
GFP+/total(After)	42.1	25.6	16.5
GFP+ After/Before	108.5	87.6	45.7

Moesin-wt transfectants was in between. These results indicated the followings. (i) Moesin-TD was detected by either anti-ERM Ab or anti-phospho-ERM Ab. (ii) Only part of Moesin-wt was phosphorylated at Thr588 in HEK293T cells.

Combined, these findings indicate that phospho-mimetic Moesin alone could induce cell rounding and inhibit cell reattachment to substrate.

Staurosporine-induced ERM dephosphorylation and cell adhesion in KG-1 cells

We already described the involvement of phospho-ERM in the rounding of adherent cells and in the inhibition of cell reattachment. Meanwhile, non-adherent cells are spherical and do not attach to substrate. We next investigated the role of phospho-ERM in the maintenance of such cell shape/adhesion-related characteristics in KG-1 cells. KG-1 cells are round non-adherent cells derived from acute myelogenous leukemia with microvilli on their surface.[24] ERM proteins such as Ezrin are localized at microvilli and spherical surface of KG-1 cells. Despite surface expression of α4β1 integrin, KG-1 cells hardly adhere to substrate even coated with GST-CS1, a ligand for α4β1 integrin.[24] However, we found that Staurosporine treatment augmented KG-1 cell adhesion to the GST-CS1-coated substrate. Significant increase of KG-1 cell attachment after washing (**Fig. 3A**) and decrease in the number of unattached KG-1 cells (**Fig. 3B**) were observed by Staurosporine treatment, indicating augmented integrin-mediated cell adhesion to substrate by Staurosporine.

Immunoblot analysis showed dose-dependent decrease of phospho-ERM by Staurosporine treatment in KG-1 cells (**Fig. 3C**). Incubation with 10 nM Staurosporine for 1h almost completely abrogated phospho-ERM, while incubation with less concentration showed lower decrease. The results showed a dose-dependent correlation between decrease of phospho-ERM and number of unattached cells (**Fig. 3B**). Immunofluorescent images of poly-L-lysine (PLL)-attached KG-1 cells also showed diminished phospho-ERM by Staurosporine treatment (Supple 3). Phospho-ERM (Supple 3) and Ezrin (**Fig. 3D**) were detected at the edge of non-treated KG-1 cells attached to PLL-coated substrate, indicating localization at the plasma membrane. However, Ezrin was mostly detected at the cytoplasm in Staurosporine-treated cells (**Fig. 3D**). These observations revealed subcellular localization of phospho-ERM at the plasma membrane of KG-1 cells and shift of Ezrin localization to the cytoplasm by dephosphorylation.

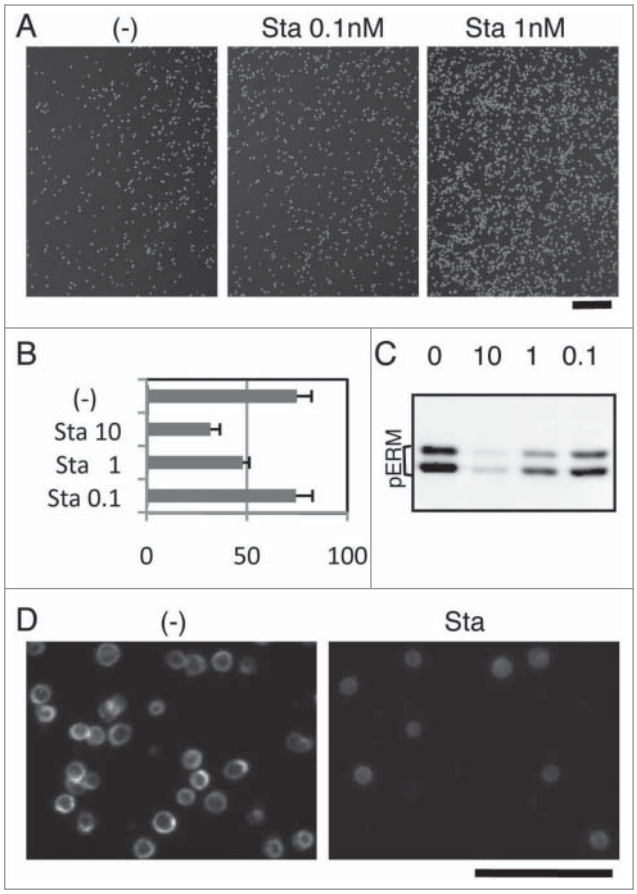

Figure 3. Staurosporine-induced ERM dephosphorylation and cell adhesion in KG-1 cells. (**A**) Staurosporine (Sta) treatment-induced adhesion of KG-1 cells. KG-1 cells were incubated in the GST-CS1-coated plate with or without Staurosporine. Images of cells remained attached to plate after wash are demonstrated. Magnification: x40. Scale bar: 400 μm. (**B**) Effect of Staurosporine on cell adhesion. Unattached cells in the adhesion assay were counted and compared. Ratios of unattached cells per total incubated cells are demonstrated by percentage. Treatment with 1nM or more Staurosporine decreased unattached cells. Concentration: nM (**C**) Immunoblot analysis with anti-phospho-ERM Ab. Lysates of Staurosporine-treated or untreated KG-1 cells were analyzed by immunoblotting. Concentrations of Staurosporine (nM) are indicated. (**D**) Immunofluorescent analysis with anti-Ezrin Ab. KG-1 cells attached to poly-L-lysine-coated coverglass chamber treated with or without 10 nM Staurosporine were analyzed by immunocytochemistry. Staining with anti-Ezrin Ab was detected at the edge of cells in untreated cells, while detected at the cytoplasm in Staurosporine-treated cells. Magnification: x200. Scale bar: 100 μm.

These findings further suggested the role of phospho-ERM in the inhibition of cell adhesion.

Subcellular localization of phosphorylated ERM proteins

Expression of phospho-mimetic Moesin mutant or Cal-A treatment induced cell body retraction, rounding and inhibition of reattachment in adherent cells. To reveal mechanisms for these phenomena, we investigated subcellular localization of phospho-ERM. First, we analyzed HEK293T transfectants by immunocytochemistry. As demonstrated in **Figure 4A**, staining with anti-phospho-ERM Ab was clearly detected at the outer edge membrane in Moesin-TD transfectants, while was hardly detected in GFP-alone transfectants. Staining with anti-Moesin Ab was also detected at the outer edge of Moesin-TD transfectants, while was detected mostly at the cytoplasm of Moesin-wt transfectants (**Fig. 4B**). These results indicated subcellular localization of phospho-mimetic Moesin at the plasma membrane of round cells.

More drastic changes were observed in Cal-A treated NIH3T3 cells. In non-treated spread cells, staining with anti-phospho-ERM Ab was detected as filopodia-like structures at cell edge in substrate-attach phase or as short microvilli on the apical surface (**Fig. 4C and D**). Meanwhile, staining with Phalloidin was observed at stress fibers, filopodia, and microvilli (**Fig. 4C and D**). Notably, phospho-ERM were hardly detected along actin stress fibers. After incubation with Cal-A, spread cell body was retracted, and bleb-like structures appeared on the side and apical surface of retracted cells (**Fig. 1A**). Staining with anti-phospho-ERM Ab and Phalloidin were detected at the cell edge and rims of bleb-like structures (**Fig. 4C and E**). This result indicated co-localization of cortical actin cytoskeleton with phospho-ERM at the inner surface of bleb-like structures. Meanwhile, actin stress fibers were largely reduced in shrunk cells. Since phospho-ERM crosslink plasma membrane and actin cytoskeleton, these observations strongly suggested the involvement of phospho-ERM in gross reorganization of actin cytoskeleton.

A few cells showed a mixed phenotype between non-treated and shrunk cells (**Fig. 4F**). The attachment site and the top parts of the cells were similar to those of non-treated cells, while cell periphery in the middle was covered with blebs. This finding suggested that Cal-A-induced cell body retraction started from the apical side of cells, especially from the side slope. Meanwhile, pretreatment with high concentration of Blebbistatin, a Myosin II inhibitor, partially inhibited Cal-A-induced bleb formation, but did not inhibit cell body retraction (**Fig. 4C**). Thus, further study is required to clarify the mechanism of Cal-A-induced cell rounding.

Most actin stress fibers disappeared in Cal-A-treated cells (**Fig. 4C and E**). Since stress fibers are connected to focal adhesions, phosphorylation status of focal adhesion kinase (FAK) was investigated to find changes in focal adhesions. As demonstrated in **Figure 4G**, phospho-Y397-FAK was reduced over time after Cal-A addition in NIH3T3 cells in a concentration and time-dependent manner. This decrease of phospho-Y397-FAK upon Cal-A treatment was correspondent with the increase of phospho-ERM (**Fig. 1B**) and with the advance of cell body retraction and rounding (**Fig. 1A** and data not shown). Since phospho-Y397-FAK is the marker of integrin-induced signaling, these findings further suggested decrease of integrin-mediated cell adhesion and signaling in Cal-A-treated cells.

Alterations of cell surface rigidity by phosphorylated ERM

Phospho-ERM as well as phospho-mimetic Moesin mutant were localized at the plasma membrane in HEK293T and NIH3T3 cells. Actin cytoskeleton was also detected at the plasma membrane of Cal-A-treated NIH3T3 cells. However, our

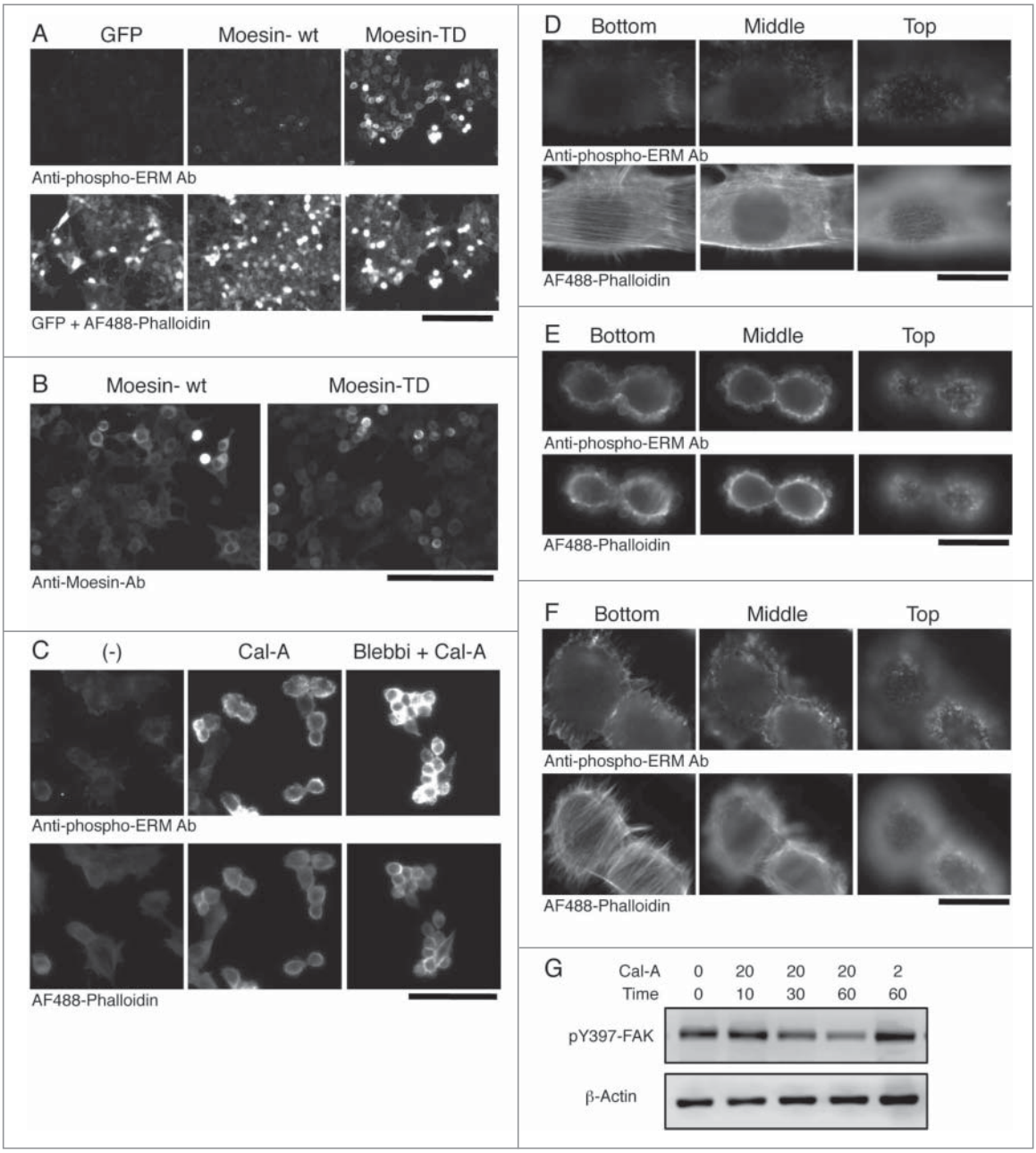

Figure 4. Subcellular localization of phospho-ERM proteins. (**A**) Immunocytochemistry of HEK293T transfectants with anti-phospho-ERM Ab. Up: fluorescent images of anti-phospho-ERM Ab. Down: fluorescent images of GFP and AF488-labeled Phalloidin. Magnification: x200. Scale bar: 200 μm. (**B**) Immunocytochemistry of HEK293T transfectants with anti-Moesin Ab. Staining with anti-Moesin Ab was detected at the edge of cells in Moesin-TD transfectants, while detected rather at the cytoplasm in Moesin-wt transfectants. Magnification: x200. Scale bar: 200 μm. (**C**) Immunocytochemistry of Cal-A-treated NIH3T3 cells. NIH3T3 cells untreated (left), treated with 20 nM Cal-A for 20 min (middle), and treated with Cal-A after Blebbistatin (Blebbi) pretreatment (right) were analyzed with anti-phospho-ERM Ab (up) and AF488-labeled Phalloidin (down). Cal-A treatment augmented phospho-ERM, induced cell body retraction and bleb formation. Fewer blebs were observed in Blebbistatin-pretreated cells. Magnification: x200. Scale bar: 200 μm. (**D**) Non-treated NIH3T3 cells. (**E, F**) Cal-A treated NIH3T3 cells. From D to F: Up: anti-phospho-ERM Ab. Down: AF488-labeled Phalloidin. Magnification: x1000. Scale bar: 20 μm. Side (**E, F**) and top (**E**) parts of Cal-A-treated cells were covered with blebs. Phospho-ERM and Phalloidin staining were detected at the rim of blebs. (**G**) Immunoblotting with anti-pY397-FAK. NIH3T3 cell lysates used in **Figure 1B** were analyzed by immunoblotting with anti-phospho-FAK (Y397) and anti-β-Actin Abs. Phospho-Y397-FAK was decreased over time after Cal-A addition to 20 nM. Concentration of Cal-A: nM, time: min.

immunocytochemical analysis with Phalloidin was not clear in HEK293T cells. Moreover, recruitment of actin cytoskeleton to plasma membrane could cause changes in physical characteristics of cell surface. Since cell shape and adhesion could be affected by such changes, we investigated cell surface stiffness by atomic force microscopy (AFM).

First, alteration of surface rigidity of HEK293T cells by Cal-A treatment was investigated by the methods described in Materials and Methods. As demonstrated in **Figure 5A**, average surface stiffness of Cal-A-treated HEK293T cells were 1.7 times higher than untreated cells.

Then, we analyzed the effect of Moesin-TD expression on cell surface rigidity. Co-transfection of HEK293T cells with 10:1 molar ratio of pCAG-Moesin-TD and pCpuro-GFP boosted surface rigidity of GFP+ cells comparing to GFP- cells (**Fig. 5B**).

These results strongly suggested augmentation of cell surface rigidity by phospho-ERM probably via the recruitment of actin cytoskeleton to plasma membrane. This increased cell surface rigidity could be involved in the formation/maintenance of spherical cell morphology and in the inhibition of cell reattachment.

Discussion

It has been well documented that cell adhesion, either cell to cell or cell to substrate, evokes various intracellular signaling by the interaction between cell adhesion molecules and their ligands. Morphology of adherent cells is generated based on the influence of such signaling from adhesion molecules. Meanwhile, non-adherent cells such as leukocytes and transiently detached adherent cells are spherical in shape. It has been speculated that cells without adhesion spontaneously form spherical shape without any signaling. However, recent studies by us and other laboratories demonstrated that: (i) phospho-ERM were observed at the plasma membrane of non-adherent cells such as peripheral T lymphocytes.[2]; (ii) phosphorylation of ERM proteins was induced by the detachment of adherent cells, while phospho-ERM were reduced by cell adhesion to substrate.[23] Thus, augmented phospho-ERM were commonly observed in the suspended cells. In this article, we artificially modified phosphorylation status of ERM proteins by several methods and investigated changes in cell shape and adhesion.

First, phosphorylation level of ERM proteins was low in spread adherent cells such as NIH3T3 or HEK293T cells. However, phospho-ERM were dramatically augmented by the treatment with a protein phosphatase inhibitor, Cal-A. This finding indicated that ERM proteins were constitutively dephosphorylated by protein phosphatases in spread adherent cells. Constitutive phosphorylation of ERM proteins by protein kinases in these cells was also indicated by this finding as well as by Staurosporine-induced decrease of phospho-ERM. Thus, ERM proteins are kept both phosphorylated and dephosphorylated in adherent cells. However, dephosphorylation of ERM proteins appears to be dominant over phosphorylation in substrate-attached adherent cells. On the other hand, phosphorylated ERM proteins are kept in rather high level in KG-1 cells, which are non-adherent and spherical cells. ERM proteins were dephosphorylated by Staurosporine in KG-1 cells, while were further phosphorylated by Cal-A treatment (data not shown). Thus, ERM proteins are kept both phosphorylated and dephosphorylated in KG-1 cells, too. However, phospho-ERM in KG-1 cells cultured in suspension appear to be kept in a rather high level. Thus, phosphorylation degree of ERM proteins is strongly regulated in cells by protein kinases and phosphatases, i.e. low in spread adherent cells and rather high in spherical non-adherent cells.

We then investigated alterations in cell shape and adhesion by the modification of ERM phosphorylation. Cal-A treatment and expression of phospho-mimetic Moesin mutant resulted in cell rounding and inhibited cell reattachment in adherent cells. Meanwhile, Staurosporine treatment abrogated phospho-ERM and augmented integrin-mediated KG-1 cell adhesion. These findings strongly suggest that higher level of phospho-ERM inhibits cell adhesion to substrate in both adherent and non-adherent cells. It induces cell rounding and maintained spherical cell shape as well.

Meanwhile, spherical cell shape is possibly involved in the regulation of cell adhesion. Non-adherent cells and detached adherent cells are spherical in shape. During adhesion process, cells change their shape from spherical to flat after initial contact with substrate (**Fig. 6**). This cell shape change increases contact area with flat substrate and results in firm adhesion. Therefore, keeping spherical shape despite initial contact impedes further increase of attachment area and consequently inhibits establishment of sound cell adhesion. We next examined possible evidence showing that high level phospho-ERM maintained spherical cell shape. Non-adherent spherical

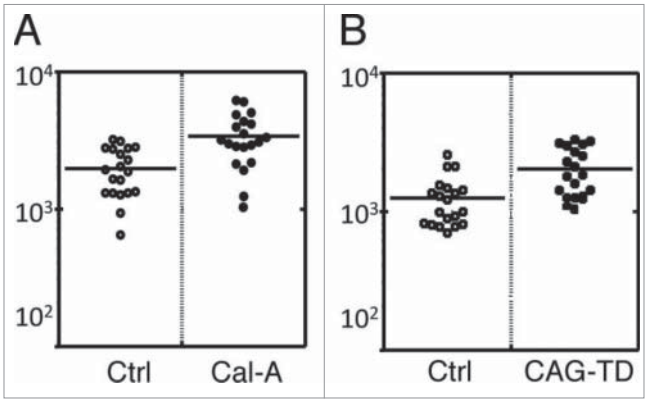

Figure 5. AFM analysis of Moesin transfectants. (**A**) AFM analysis of Cal-A-treated HEK293T cells. Average Young's modulus of Cal-A treated and non-treated control (Ctrl) cells were 3397 and 1979 Pa, respectively. (**B**) AFM analysis of Moesin-TD transfectants. Average Young's modulus of GFP+ transfectants and GFP- cells were 2033 and 1251 Pa, respectively. The lower Young's modulus of GFP- cells compared to control cells in A is due to the effect of lipofection.

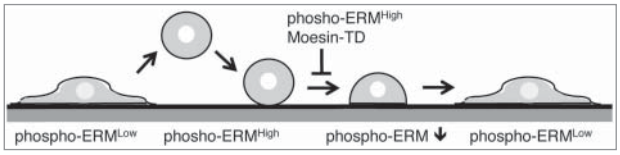

Figure 6. Simplified schema of cell adhesion. Transition of cell shape and phosphorylation status of ERM during detachment and reattachment of adherent cells is depicted. Moesin-TD expression or keeping ERM highly phosphorylated inhibits proceeding of cell adhesion. Cell surface structures such as filopodia, microvilli and bleb are not shown.

cells such as lymphocytes and KG-1 cells were rather rich in phospho-ERM. SDF-1 treatment led to dephosphorylation of ERM and loss of spherical cell shape, while Moesin-TD expression partially inhibited SDF-1-induced cell shape change.[2] Moesin-TD transfectants as well as Cal-A-treated cells were spherical, especially when detached by trypsinization. Moesin-TD expressed cells remained spherical for a few days (data not shown). Both Moesin-TD transfectants and Cal-A-treated cells showed higher cell surface rigidity by AFM, indicating more resistant to deformation. Thus, phosphomimetic ERM mutants as well as forced phosphorylation of ERM probably maintain spherical cell shape, supporting the hypothesis that phospho-ERM inhibit cell adhesion via keeping spherical cell shape. If this is the case, adhesion of detached adherent cells to substrate occurs in a sequential fashion as follows (**Fig. 6**): (1) Initial contact with substrate, (2) dephosphorylation of ERM proteins around the contact sites, (3) cell shape change, and (4) development of further attachment. Meanwhile, non-adherent cells such as lymphocytes and KG-1 cells do not attach to substrate under the normal culture conditions. Such inhibition of cell adhesion can be explained by the lack of either initial attachment or adhesion-induced dephosphorylation of ERM. In addition, Staurosporine treatment dephosphorylated phospho-ERM and augmented cell adhesion in KG-1 cells. These results suggest that low dephosphorylation of phospho-ERM is one of the potential reasons why non-adherent cells stay unattached.

There are other possible mechanisms for inhibition of cell adhesion by phospho-ERM. Adhesion inhibitory transmembrane proteins such as CD43 are linked to cortical actin cytoskeleton by phospho-ERM in leukocytes.[27] Phospho-ERM scatter inhibitory proteins on the whole cell surface and inhibit cell adhesion. Certain signaling such as T cell receptor signaling induces dephosphorylation of ERM proteins and promotes adhesion of T cells to antigen presenting cell.[3,4,27] Thus, in non-adherent cells such as T lymphocytes, complex of adhesion inhibitory molecules, phospho-ERM, and cortical actin cytoskeleton reversibly regulates cell adhesion. However, such ERM-binding adhesion-inhibitory cell surface mucins appear to be not highly expressed in adherent cells, suggesting a different mechanism for phospho-ERM-mediated inhibition of cell adhesion. As the other possibility, clustering of surface adhesion molecules may be inhibited by phospho-ERM through organization of cell surface structure. In our previous report, immunostaining of β1 integrin on microvilli was patchy in KG-1 cells.[24] This datum suggested that adhesion molecules are sparsely localized on cell surface. Therefore, inhibition of adhesion molecule clustering by membrane-linked cortical actin cytoskeleton and/or cell surface structure may result in failed cell adhesion. We believe one or a combination of these mechanisms is involved in the inhibition of cell adhesion in the cells rich in phospho-ERM.

In this article, we also showed rounding of adherent cells either by Cal-A-treatment or by Moesin-TD expression. Cal-A treatment induced rapid retraction of spread cell body with massive bleb formation. This bleb formation appeared to start from side parts of cells, and then expanded to apical parts. Bleb formation at the side and apical parts during cell retraction possibly induces relocation of cellular elements toward central and upper regions. Previous report about serial cell shape changes from spread to bleb formation to round by Cal-A treatment further indicates the involvement of bleb formation during cell rounding.[28] The initial step of bleb formation is induced by the local increase of intracellular hydrostatic pressure, which is generated by myosin.[29,30] Meanwhile, phosphorylation of myosin regulatory light chain was augmented by Cal-A treatment.[25,26] Thus, bleb formation in Cal-A-treated cells can be the result of augmented phosphorylation of myosin regulatory light chain. Meanwhile, previous reports proposed the involvement of phospho-ERM in the retraction of blebs by recruiting actin cytoskeleton.[21,31] Bending rigidity of the underlying cortex was increased during bleb retraction,[30] further suggesting the involvement of cortical actin cytoskeleton in bleb retraction. We also observed increase of cell surface rigidity either by Cal-A treatment or Moesin-TD expression. Thus, bleb formation and phospho-ERM can be involved in Cal-A-induced cell rounding. However, pre-treatment with high concentration of Blebbistatin reduced Cal-A-induced bleb formation, but did not inhibit cell retraction and rounding. Thus, further studies are needed to confirm the roles of bleb formation and phospho-ERM in cell rounding.

Meanwhile, Moesin-TD expression needs longer time for cell rounding than Cal-A treatment. This can be due to the initial time required for Moesin-TD expression, but can be a different cell-rounding mechanism. Adherent cells undergo cell body retraction, rounding, and bleb formation during mitosis.[21] Since spherical cell shape was maintained in Moesin-TD transfectants, expression of phospho-mimetic Moesin possibly inhibits re-spreading of round mitotic cells and augments round-shaped cells. Then, what is the potential mechanism for phospho-ERM/Moesin-TD to maintain spherical cell shape? Colocalization of phospho-ERM/Moesin-TD and polymerized actin at the plasma membrane of round cells strongly suggest recruitment of actin cytoskeleton to the cell cortex by phospho-ERM. In combination with the decrease of actin stress fibers in Cal-A-treated NIH3T3 cells, reorganization of actin cytoskeleton in the vicinity of the plasma membrane was induced by phospho-ERM. In Cal-A-treated cells, Phalloidin-staining was detected at the plasma membrane such as inner surface of bleb rim. To cover the inner surface of such spherical 3-dimensional protrusion, 2-dimensional actin networks are necessary.[30,31] Such phospho-ERM-cortical actin networks at the inner surface augments cell surface rigidity by providing extra structural support for plasma membrane,[30] which in turn increase resistance to cell shape deformation. [32] Furthermore, 2-dimentional contractile acto-myosin structures can form membrane curvatures,[33] suggesting formation/maintenance of spherical cell surface. Thus, phospho-ERM and reorganized actin cytoskeleton possibly maintain cell surface architecture by backing plasma membrane. If this is the case, modification of phosphorylation status of ERM and reorganization of actin cytoskeleton are essential to alter spherical cell shape.

In summary, cell shape and adhesion are regulated by phosphorylation status of ERM proteins in both adherent and suspended cells. Upholding ERM proteins in phosphorylated state leads to the inhibition of cell adhesion to substrate, paradoxically indicating the

significance of ERM dephosphorylation in cell adhesion process. Given that at least one of the ERM proteins is expressed in all metazoans, regulation of ERM phosphorylation/dephosphorylation could be one of the key biological events in multicellular organisms.

Materials and Methods

Cells and reagents

HEK293T, NIH3T3, KG-1 cells and their culture were described previously.[24] Rabbit anti-ERM (#3142) and anti-phospho-ERM (#3149) antibodies (Abs) were obtained from Cell Signaling Technology. This anti-phospho ERM Ab is reactive against human phospho-Ezrin (Thr567)/ Radixin (Thr564)/ Moesin (Thr558) and phospho-ERM of other species, while anti-ERM Ab is reactive against human and mouse Ezrin, Radixin and Moesin. Mouse anti-Moesin (610401) and anti-Ezrin (610603) monoclonal Abs were obtained from BD Biosciences, Alexa Fluor (AF) 546-labeled anti-Mouse Ig, anti-Rabbit Ig Abs, AF488-labeled Phalloidin, and anti-phospho-FAK (Y397) (44–624) were from Life Technologies. Calyculin A (Cal-A), Staurosporine and Blebbistatin (-) were obtained from Wako, while poly-L-lysine (PLL, P-8920) and anti-β-Actin Ab (A-5316) was from Sigma-Aldrich.

DNA

Human Moesin cDNA was cloned by RT-PCR. The cDNA encoding Moesin Thr558Asp was generated by site directed mutagenesis. A mammalian expression vector, pCLN (Imgenex), was modified to replace neomycin resistant gene with GFP gene to generate pCGFP vector. A Moesin cDNA was subcloned into pCGFP. In pCGFP-Moesin vectors, Moesin and GFP genes are on the same plasmid, but are driven by different promoters. pCAG vector was generated with CAG promoter. Transfection of expression vectors into HEK293T cells were performed with LipofectAmine 2000 (Life Technologies). Production of GST-CS1 peptide was described previously.[34]

Cell rounding assay

NIH3T3 and HEK293T cells were incubated in culture media containing Cal-A for the indicated time. After images were taken, cells were subjected to reattachment assay, and cellular lysates were obtained for immunoblotting. For double treatment, Staurosporine or Blebbistatin was added 30 min before Cal-A treatment. Meanwhile, transfected cells were analyzed at 42 to 45 hrs after the start of transfection for imaging and reattachment assay.

Cell adhesion assay

For reattachment assay, NIH3T3 and HEK293T cells were trypsinized, washed, re-suspended in culture media, and incubated in CO_2 incubator for 1 h. For Cal-A treatment, cells were pre-incubated for 30 min with 10 nM Cal-A before trypsinization and reincubated with 10 nM Cal-A. After incubation, unattached cells were washed off and counted. Images of cells remained attached to substrate were captured as reattached cells.

For adhesion assay of KG-1, cells were incubated in the plate coated with GST–CS1 peptide in the culture media with or without Staurosporine for 3h. After incubation, cells that did not adhere to substrate were removed by washing and counted as non-attached cells. Meanwhile, images of cells remained attached to substrate after wash were captured as attached cells. For coating, petri-plate (Greiner) was incubated with PBS containing 1 μg/ml GST-CS1 peptide overnight in CO_2 incubator, while coverglass chambers (IWAKI) were incubated with PBS containing 0.001 % PLL.

All cell counts were performed in triplicate, and average values are shown with standard deviation.

Immunoblotting

Cells were lysed in lysis buffer containing 1% CHAPS (DOJINDO), sonicated, and subjected to immunoblot analysis as described previously.[23] Lysates from same number of cells were electrophoresed in lanes of each blot. Blocking and incubation with primary antibodies were performed in TBS containing 5% BSA. Analysis was performed with LAS4000mini (Life Technologies) or C-Digit (LI-COR).

Microscopy

For phase contrast and fluorescent microscopy for GFP, images of cells on culture dish were taken. For immunocytochemistry, adherent cells were grown on coverglass chambers and treated as described previously,[24] while KG-1 cells were incubated for 30 min with or without Staurosporine in PLL-coated coverglass chambers before fixation. Both phase contrast and fluorescent microscopy were performed by IX70 (OLYMPUS) and ORCA-ER (Hamamatsu Photonics). Number of cells in the images was counted.

Flowcytometry

HEK293T transfectants were analyzed by flowcytometry with FACS Calibur (BD Biosciences) as described previously.[24]

AFM assay

HEK293T cells cultured on 35 mm dishes in medium were manipulated by AFM (Nanowizard I; JPK Instruments AG) equipped with a plate heater at 37°C. Integration of the optical microscopy (IX-71; Olympus) and AFM allows the probe to be placed on a target region of the cell surface. For the analysis with Cal-A treatment, Cal-A was added to culture media 30 min before the start of AFM assay. For the analysis of transfectants, HEK293T cells were transfected with pCAG-Moesin-TD and pCpuro-GFP by LipofectAmine 2000 for 16 h. Then, cells were trypsinized, replated on 35 mm dishes and incubated for 24h. Combination of fluorescence microscopy and AFM enabled us to identify and measure transfectants. The AFM probe indented the cell surface on the nuclear region with a loading force of up to 1 nN and approaching velocity of 5 μm/s. The Young's modulus of the cell was calculated using the Hertz model.[35] The force distance curve for a region up to about 500 nm of cell surface indentation was fitted using JPK data

processing software (JPK Instruments AG) as:

$$F = \frac{E}{1-\nu^2}\,\frac{\tan\alpha}{\sqrt{2}}\,\delta^2$$

where F is force, δ is depth of the probe indentation, ν is Poisson's ratio (0.5), α is half-angle to the face of the pyramidal probe (20°), and E is Young's modulus. More than 20 cells were used per experiment, and 25 points were examined on the surface of each cell. Since distribution of the Young's modulus values of a cell exhibited a log-normal pattern,[36] the average of the Young's modulus was used to show cell surface stiffness in each condition.

Disclosure of Potential Conflicts of Interest

No potential conflicts of interest were disclosed.

Acknowledgments

We thank Dr. Kenjiro Kamiguchi for the GST-CS-1 vector, Dr. Junichi Miyazaki for CAG promoter, and Dr. Takanori Kihara for helpful discussion.

Funding

This work was in part supported by Grants-in-Aid for Scientific Research on Innovative Areas "Nanomedicine Molecular Science" (No 2306) from the Ministry of Education, Culture, Sports, Science and Technology of Japan.

Supplemental Material

Supplemental data for this article can be accessed on the pub lisher's website.

References

1. Serrador JM, Alonso-Lebrero JL, del Pozo MA, Furthmayr H, Schwartz-Albiez R, Calvo J, Lozano F, Sánchez-Madrid F. Moesin interacts with the cytoplasmic region of intercellular adhesion molecule-3 and is redistributed to the uropod of T lymphocytes during cell polarization. J Cell Biol 1997; 138:1409-23; PMID:9298994; http://dx.doi.org/10.1083/jcb.138.6.1409
2. Brown MJ, Nijhara R, Hallam JA, Gignac M, Yamada KM, Erlandsen SL, Delon J, Kruhlak M, Shaw S. Chemokine stimulation of human peripheral blood T lymphocytes induces rapid dephosphorylation of ERM proteins, which facilitates loss of microvilli and polalization. Blood 2003; 102:3890-9; PMID:12907449; http://dx.doi.org/10.1182/blood-2002-12-3807
3. Delon J, Kaibuchi K, Germain RN. Exclusion of CD43 from the immunological synapse is mediated by phosphorylation-regulated relocation of the cytoskeletal adaptor moesin. Immunity 2001; 15:691-701; PMID:11728332; http://dx.doi.org/10.1016/S1074-7613(01)00231-X
4. Roumier A, Olivo-Marin JC, Arpin M, Michel F, Martin M, Mangeat P, Acuto O, Dautry-Varsat A, Alcover A. The membrane-microfilament linker ezrin is involved in the formation of the immunological synapse and in T cell activation. Immunity 2001; 15:715-28; PMID:11728334; http://dx.doi.org/10.1016/S1074-7613(01)00225-4
5. Fiévet B, Louvard D, Arpin M. ERM proteins in epithelial cell organization and functions. Biochem Biophys Acta 2007; 1772:653-60; http://dx.doi.org/10.1016/j.bbamcr.2006.06.013
6. Arpin M, Chirivino D, Naba A, Zwaenepoel I. Emerging role for ERM proteins in cell adhesion and migration. Cell Adh Migr 2011; 5:199-206; PMID:21343695; http://dx.doi.org/10.4161/cam.5.2.15081
7. Niggli V, Rossy J. Ezrin/radixin/moesin: Versatile controllers of signaling molecules and of the cortical cytoskeleton. Int J Biochem Cell Biol 2008; 40: 344-9; PMID:17419089; http://dx.doi.org/10.1016/j.biocel.2007.02.012
8. Yonemura S, Nagafuchi A, Sato N, Tsukita S. Concentration of an integral membrane protein, CD43 (Leukosialin, Sialophorin), in the cleavage furrow through the interaction of its cytoplasmic domain with actin-based cytoskeletons. J Cell Biol 1993; 120:437-49; PMID:8421057; http://dx.doi.org/10.1083/jcb.120.2.437
9. Niggli V, Andréoli C, Roy C, Mangeat P. Identification of phosphatidylinositol-4,5-biphosphate-binding domain in the N-terminal region of ezrin. FEBS Lett 1994; 376:172-6; http://dx.doi.org/10.1016/0014-5793(95)01270-1
10. Hirao M, Sato N, Kondo T, Yonemura S, Monden M, Sasaki T, Takai Y, Tsukita S, Tsukita S. Regulation mechanism of ERM (Ezrin/Radixin/Moesin) protein/plasma membrane association: possible involvement of phosphatidylinositol turnover and Rho-dependent signaling pathway. J Cell Biol 1996; 13:37-51; http://dx.doi.org/10.1083/jcb.135.1.37
11. Pearson MA, Reczek D, Bretscher A, Karplus PA. Structure of the ERM protein Moesin reveals the FERM domain fold masked by an extended actin binding tail domain. Cell 2000; 101:259-270; PMID:10847681; http://dx.doi.org/10.1016/S0092-8674(00)80836-3
12. Hamada K, Shimizu T, Matsui T, Tsukita S, Tsukita S, Hakoshima T. Structural basis of the membrane-targeting and unmasking mechanisms of the radixin FERM domain. EMBO J 2000; 19:4449-62; PMID:10970839; http://dx.doi.org/10.1093/emboj/19.17.4449
13. Ben-Aissa K, Patino-Lopez G, Belkina NV, Maniti O, Rosales T, Hao J-J, Kruhlak MJ, Knutson JR, Picart C, Shaw S. Activation of Moesin, a protein that links actin cytoskeleton to th plasma membrane, occurs by phosphatidylinositol 4,5-bisphosphate (PIP2) binding sequentially to two sites and releasing an autoinhibitory linker. J Biol Chem 2012; 287:16311-23; PMID:22433855; http://dx.doi.org/10.1074/jbc.M111.304881
14. Bretshcer A. Regulation of cortical structure by the ezrin-radixin-moesin protein family. Curr Opin Cell Biol 1999; 11:109-16; PMID:10047517; http://dx.doi.org/10.1016/S0955-0674(99)80013-1
15. Tsukita S, Yonemura S. Cortical actin organization: lessons from ERM (Ezrin/Radixin/Moesin) proteins. J Biol Chem 1999; 274:34507-10; PMID:10574907; http://dx.doi.org/10.1074/jbc.274.49.34507
16. Nakamura F, Amieva MR, Furthmayr H. Phosphorylation of threonine 558 in the carboxyl-terminal actin-binding domain of moesin by thrombin activation of human platelets. J Biol Chem 1995; 270:31377-85; PMID:8537411; http://dx.doi.org/10.1074/jbc.270.52.31377
17. Matsui T, Maeda M, Doi Y, Yonemura S, Amano M, Kaibuchi K, Tsukita S, Tsukita S. Rho-kinase phosphorylates COOH-terminal Threonines of Ezrin/Radixin/Moesin (ERM) proteins and regulates their head to taio association. J Cell Biol 1998; 140:647-57; PMID:9456324; http://dx.doi.org/10.1083/jcb.140.3.647
18. Nakamura F, Amieva MR, Hirota C, Mizuno Y, Furthmayr H. Phosphorylation of 558T of moesin detected by site-specific antibodies in RAW264.7 macrophages. Biochem Biophys Res Commun 1996; 226: 650-6; PMID:8831671; http://dx.doi.org/10.1006/bbrc.1996.1410
19. Nakamura F, Huang L, Pestonjamasp K, Luna EJ, Furthmayr H. Regulation of F-actin binding to platelet moesin in vitro by both phosphorylation of Threonine 558 and polyphosphatidylinositides. Mol Biol Cell 1999; 10:2669-85; PMID:10436021; http://dx.doi.org/10.1091/mbc.10.8.2669
20. Louvet-Vallée S. ERM proteins: From cellular architecture to cell signaling. Biol Cell 2000; 92:305-16; http://dx.doi.org/10.1016/S0248-4900(00)01078-9
21. Kunda P, Pelling AE, Liu T, Baum B. Moesin controls cortical rigidity, cell rounding, and spindle morphogenesis during mitosis. Curr Biol 2008; 18:91-101; PMID:18207738; http://dx.doi.org/10.1016/j.cub.2007.12.051
22. Carreno S, Kouranti I, Glusman ES, Fuller MT, Echard A, Payre F. Moesin and its activating kinase Slik are required for cortical stability and microtubule organization in mitotic cells. J Cell Biol 2008; 180:739-46; PMID:18283112; http://dx.doi.org/10.1083/jcb.200709161
23. Yamane J, Ohnishi H, Sasaki H, Narimatsu H, Ohgushi H, Tachibana K. Formation of microvilli and phosphorylation of ERM family proteins by CD43, a potent inhibitor for cell adhesion. Cell Adh Migr 2011; 5:119-32; PMID:21045567; http://dx.doi.org/10.4161/cam.5.2.13908
24. Ohnishi H, Sasaki H, Nakamura Y, Kato S, Ando K, Narimatsu H, Tachibana K. Regulation of cell shape and adhesion by CD34. Cell Adh Migr 2013; 7:426-33; PMID:24036614; http://dx.doi.org/10.4161/cam.25957
25. Chartier L, Rankin LL, Allen RE, Kato Y, Fusetani N, Karaki H, Watabe S, Hartshorne DJ. Calyculin-A inceases the level of protein phosphorylation and changes the shape of 3T3 fibroblasts. Cell Motil Cytoskeleton 1991; 18:26-40; PMID:1848484; http://dx.doi.org/10.1002/cm.970180104
26. Suzuki A, Itoh T. Effects of calyculin A on tension and myosin phosphorylation in skinned smooth muscle of the rabbit mesenteric artery. Br J Pharmacol 1993; 109:703-12; PMID:8395295; http://dx.doi.org/10.1111/j.1476-5381.1993.tb13631.x
27. Shaw AS. FERMing up the synapse. Immunity 2001; 15:683-6; PMID:11728330; http://dx.doi.org/10.1016/S1074-7613(01)00237-0
28. Leung YM, Kwan TK, Kwan CY, Daniel EE. Calyculin A-induced endothelial cell shape changes are independent of ; $Ca^{2+}{}_i$ elevation and may involve actin polymerization. Biochem Biophys Acta 2001; 1589:93-103; http://dx.doi.org/10.1016/S0167-4889(02)00161-1
29. Dai J, Scheetz MP. Membrane tether formation from blebbing cells. Biophys J 1999; 77:3363-70; PMID:10585959; http://dx.doi.org/10.1016/S0006-3495(99)77168-7
30. Charra GT, Coughlin M, Mitschison TJ, Mahadevan L. Life and times of a cellular bleb. Biophys J 2008; 94:1836-53; PMID:17921219; http://dx.doi.org/10.1529/biophysj.107.113605
31. Charras GT, Hu C-K, Coughlin M, Mitchison TJ. Reassembly of contractile actin cortex in cell blebs. J Cell Biol 2006; 175:477-90; PMID:17088428; http://dx.doi.org/10.1083/jcb.200602085

32. Gilden J, Krummel MF. Control of cortical rigidity by the cytoskeleton: emerging roles for septins. Cytoskeleton 2010; 67:477-86; PMID:20540086
33. Lecuit T, Lenne PF. Cell surface mechanics and the control of cell shape, tissue patterns and morphogenesis. Nat Rev Mol Cell Biol 2007; 8:633-44; PMID:17643125; http://dx.doi.org/10.1038/nrm2222
34. Kamiguchi K, Tachibana K, Iwata S, Ohashi Y, Morimoto C. Cas-L is required for beta 1 integrin-mediated costimulation in human T cells. J Immunol 1999; 163:563-8; PMID:10395641
35. Hertz H. Ueber die Berührung fester elastischer Körper. J Reine Angew Math 1882; 92:156-71.
36. Haghparast SMA, Kihara T, Shimizu Y, Yuba S, Miyake J. Actin-based biomechanical features of suspended normal and cancer cells. J Biosci Bioeng 2013; 116:380-5; PMID:23567154; http://dx.doi.org/10.1016/j.jbiosc.2013.03.003